

Design of Supported Nanoparticles in Ionic Liquid Medium and Its Photocatalytic Applications

**A Dissertation
Submitted in partial fulfillment**

**FOR THE DEGREE
OF
*MASTER OF SCIENCE IN CHEMISTRY***

UNDER THE ACADEMIC AUTONOMY
NATIONAL INSTITUTE OF TECHNOLOGY, ROURKELA

By
Monali Mishra

Under the Guidance of
Dr. Priyabrata Dash



**DEPARTMENT OF CHEMISTRY
NATIONAL INSTITUTE OF TECHNOLOGY
ROURKELA – 769008
ODISHA**

May, 2014

CERTIFICATE

Dr.Priyabrat Dash
Assistant Professor
Department of Chemistry
NIT, Rourkela-ODISHA



*This is to certify that the dissertation entitled “Design of Supported Nanoparticles in Ionic Liquid Medium and Its Photocatalytic Applications” being submitted by **Monali Mishra** to the Department of Chemistry, National Institute of Technology, Rourkela, Odisha, for the award of the degree of Master of Science in Chemistry is a record of bonafide research work carried out by her under my supervision and guidance. I am satisfied that the dissertation report has reached the standard fulfilling the requirements of the regulations relating to the nature of the degree.*

Rourkela-769008

Date- 6th May 2014

Dr. Priyabrat Dash

(Supervisor)

ACKNOWLEDGEMENTS

First of all, I am thankful to my guide Dr. Priyabrat Dash who untiringly assisted me in my experiment and enhanced my knowledge base by making me aware about this experiment. My training would not have been successfully completed without the firm guidance of my guide who supervised me in my experiments.

I like to thank all faculty members of the Department of chemistry, who have always inspire me to work hard and helped me to learn new concepts and experiments during my stay at NIT, Rourkela.

I would like to thank my parents for their unconditional love and support. They have helped me in every situation throughout my life, I am grateful for their support.

I would like to accord my sincere gratitude to Miss Basanti Ekka, Miss Lipeeka Rout and Mr. Aniket Kumar for their valuable suggestions, guidance in carrying out experiments. Finally, I would like to thank all my lab mates Jyoshna and Jhuma for all fun times we had together in the lab.

Finally I would like to thank all my friends for their support and the great almighty to shower his blessing on us and making dreams and aspirations.

Monali Mishra

ABSTRACT

In this project, monometallic Ag nanoparticle doped titania was synthesized via nanoparticle encapsulation method using [BMIM]PF₆ ionic liquid. The material was thoroughly characterized by Fourier transform infrared spectroscopy (FTIR), X-ray diffraction (XRD), Scanning electron microscope (SEM), Energy Dispersive X-ray (EDX) Spectroscopy and UV-Vis spectroscopy. Efficiency of the catalyst was evaluated on photodegradation of methylene blue (MB) dye under visible light irradiation. Results shows that Ag-doped titania in ionic liquid exhibited much better photodegradation (96%) as compared to Ag-doped titania in methanol medium (65%) in 210 min.

CONTENTS

		PAGE
CERTIFICATE		ii
ACKNOWLEDGEMENTS		iii
ABSTRACT		iv
TABLE OF CONTENTS		v-vi
LIST OF FIGURES		vii
CHAPTER 1	INTRODUCTION	
1.1	General Introduction	1-2
1.2	Monometallic Nanoparticle Catalysts	2
1.2.1	Chemical Reduction Method	3
1.2.2	Thermal and Decomposition Method	3
1.2.3	Electrochemical Method	3
1.3	Metal Oxides	4
1.3.1	Doping of Metal Oxides	4
1.4	Ionic Liquids	4-5
1.5	Photocatalysis	5-6
1.6	Ionic Liquid for Metal Oxide Synthesis	6-7
1.7	Objectives of Present Study	7
CHAPTER 2	MATERIALS AND METHODS	
2.1	Materials	8
2.2	Synthesis	8-
2.2.1	Synthesis of [BMIM]PF ₆ Ionic Liquid	8-9
2.2.2	Synthesis of Pure Titania in [BMIM]PF ₆ Ionic Liquid	10
2.2.3	Synthesis of Ag-Doped Titania in [BMIM]PF ₆ Ionic Liquid	10

2.3	Photocatalytic Studies	10-11
2.3.1	Instrumentation	10-11
2.3.2	Photocatalysis Measurements	11
2.4	Characterization of Catalysts	11-12
CHAPTER 3	RESULTS AND DISCUSSION	
3.1	UV-Vis Study	13
3.2	FTIR Study	13-14
3.3	SEM/EDX Study	14-15
3.4	XRD Study	15-16
3.5	Photocatalysis	16-17
CHAPTER 4	CONCLUSIONS AND FUTURE WORK	18
CHAPTER 5	REFERENCES	19-20

List of Figures

Fig. 1	Schematic illustration of preparative methods of metal nanoparticles.	2
Fig. 2	Ball and stick model of crystal structures of i) Rutile ii) Anatase and iii) Brookite TiO ₂ .	4
Fig. 3	Schematic diagram of a photocatalytic reaction.	6
Fig. 4	NMR spectra of 1-butyl-3-methylimidazolium chloride.	9
Fig. 5	NMR spectra of 1-butyl-3-methylimidazolium hexafluorophosphate.	9
Fig. 6	Photocatalysis set-up.	11
Fig. 7	UV-Vis spectra of 1-butyl-3-methylimidazolium hexafluorophosphate ionic liquid.	13
Fig. 8	FTIR of (a) Ag-doped TiO ₂ , and (b) Pure TiO ₂ in [BMIM]PF ₆ ionic liquid.	14
Fig. 9	SEM/EDX spectra of Pure TiO ₂ in [BMIM]PF ₆ ionic liquid.	14
Fig. 10	SEM/EDX spectra of Ag-doped TiO ₂ in [BMIM]PF ₆ ionic liquid.	15
Fig. 11	XRD plot of (a) Pure TiO ₂ , and (b) Ag-doped TiO ₂ in [BMIM]PF ₆ ionic liquid.	15
Fig. 12	Photocatalytic degradation of methylene blue over (a) Ag-doped TiO ₂ in [BMIM]PF ₆ ionic liquid, and (b) Ag-doped TiO ₂ in methanol medium.	16
Fig. 13	Change in colour of methylene blue after degradation under visible light using Ag-doped TiO ₂ catalyst.	17

Chapter-1

INTRODUCTION

1.1 General Introduction

Nanoparticles are the fundamental building blocks of nanotechnology. Nanoparticles are particles which range in size from 1 nm to 100 nm having specific physical and chemical properties that are intermediate between those of the atomic element from which they are composed and to those of the bulk metals.¹ Due to their larger surface area to volume ratio and unresidual energy, nanoparticles have high catalytic activity in various reactions.² The common metals which are used in the catalytic process include Ag, Au, Sn, Pd, Pt, Ru, Rh, Ni and Cu. For better performance of nanoparticles in catalysis, it is important to have nanoparticles with controlled size, shape, and composition. They can have high ratio of atoms on their surface. Nanoparticles have distinct properties such as electronic, magnetic, catalytic and optical properties which are different from those of bulk metals. Being very small in size nanoparticles have more defects *i.e.* more edges and kinks compared to larger particles. Nanoparticles may consist of identical atoms, molecules and two or more different species. They have distinct properties from those of individual atoms and molecules or bulk matter.³ Mainly metal nanoparticles are divided into two groups monometallic and bimetallic.

Silver nanoparticles are found to be a very good media for catalytic process such as photocatalytic degradation, self-cleaning, and reactive black colour decolourisation.⁴ Silver nanoparticles have unique optical, electrical, and thermal properties which are being incorporated into products that range from photovoltaic to biological and chemical sensors. Examples include conductive inks, pastes and fillers which utilize silver nanoparticles for their high electrical conductivity, stability, and low sintering temperatures. Additional applications include molecular diagnostics and photonic devices, which take advantage of the novel optical properties of these nanomaterials. An increasingly common application is the use of silver nanoparticles for antimicrobial coatings, and many textiles, keyboards, wound dressings, and biomedical devices now contain silver nanoparticles that continuously release a low level of silver ions to provide protection against bacteria.⁵ In recent years titania was considered as the most suitable candidate photocatalysts due to its stability of chemical structure, biocompatibility, strong oxidizing power, non-toxicity and low cost.⁶ The role of supported nanoparticle in titania is that it offers a way to trap the charge carriers thus improving the photocatalytic efficiency of the catalyst. This report deals with the synthesis of

silver doped titania using ionic liquid as a novel media and its application in photodegradation of methylene blue under visible light irradiation.

1.2 Monometallic Nanoparticle Catalysts

Commonly, transition metals which are not prone to oxidation are mainly used for catalysis. The most commonly used transition metals, which are used for catalysis includes mostly Pd, Pt, Cu, Ni and Rh (there are many others also).⁵ For better performance in catalysis nanoparticles should have distinct properties such as small size, shape and composition. The above parameters can be obtained by following proper synthetic methods. Normally, two synthetic process are used for metal nanoparticle synthesis such as, (i) subdivision of metallic aggregates (physical method) and (ii) nucleation and growth of metallic nanoparticles (chemical method).⁷ Among these methods chemical methods are found to be better synthetic method than physical method as nanoparticles synthesized by physical method gives broad particle size (typically particle size greater than 10 nm) and also difficult to reproduce on regular basis.⁸ Chemical process is commonly used for synthesizing metal nanoparticles as it provides better control over particle size, control over aggregation and also in composition. There are mainly three major routes used for chemical synthesis of transition metal nanoparticles: (1) chemical reduction of metallic salts, (2) thermal and photochemical decomposition of metal complexes, and (3) electrochemical reduction of metallic salts.

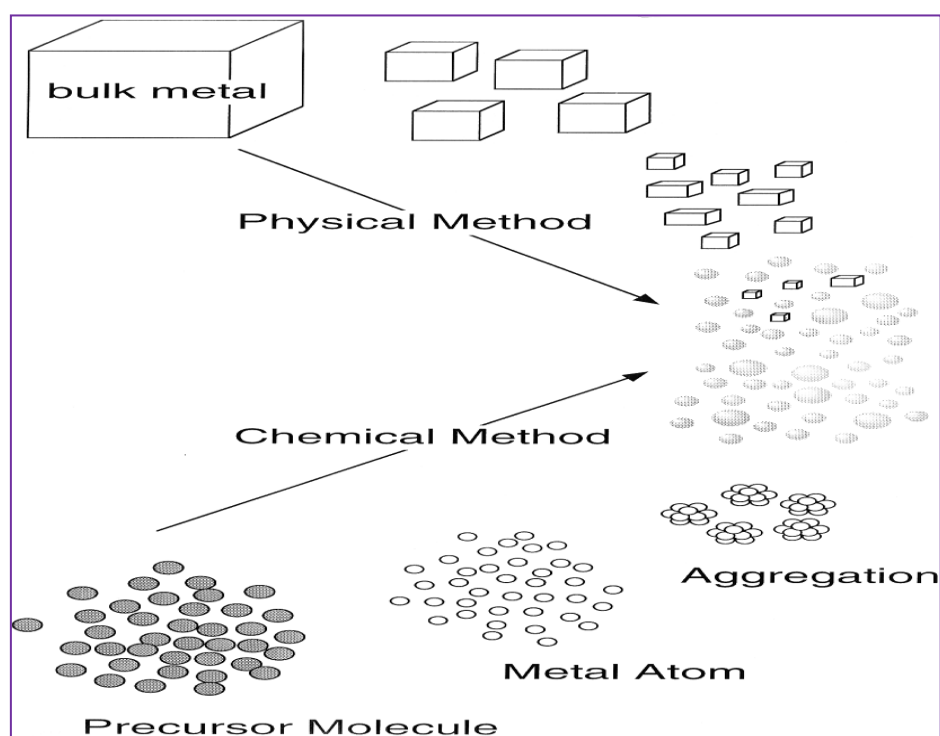


Fig. 1. Schematic illustration of preparative methods of metal nanoparticles.⁸

1.2.1 Chemical Reduction Method

In this method, metal ions are reduced to zero valent state and co-ordination of stabilizing polymer to metal nanoparticles. This method involves the reduction of a metal salt with a strong reducing agent in the presence of a stabilizer. Commonly used reducing agents include hydrides such as sodium borohydride, hydrazine, gases such as molecular hydrogen or carbon monoxide, as well as other reagents such as sodium citrate and alcohol solvents. The first reported reducing agent used for Au nanoparticle synthesis was phosphorus, which was used by Faraday to reduce AuCl_4^- ions.⁹

NaBH_4 or KBH_4 reduction methods have been widely used for the synthesis of Au, Ag, Pt, Pd and Cu nanoparticles.¹⁰ The chemical reduction have following advantages: i) the method is very simple and reproducible, ii) particle size of the obtained metal nanoparticles is small with narrow size distribution, iii) size of particle can be controlled by altering the preparative condition such as varying the concentration of metals, iv) the obtained colloidal dispersion of metal nanoparticle show a high catalytic activity, and v) the obtained colloidal dispersion are stable and no precipitates normally observed for years.⁸

1.2.2 Thermal and Photochemical Decomposition

Thermal decomposition involves pyrolysis of precursors in high boiling solvents at high temperature of ten in excess of 250-300 °C but the main disadvantage of this process is that under such condition, isolating highly reactive and unstable nanocrystal phases can be challenging. Photochemical method facilitates the generation isolation and study of metastable nanomaterial having unusual size, composition and morphology. Light induced reaction proceeds through alternative pathways at low temperature.¹¹

1.2.3 Electrochemical Reduction

Electricity is used as the driving or controlling force. Electrochemical synthesis is achieved by passing an electric current between two electrodes separated by electrolyte. The main advantages of electrochemical techniques includes avoidance of vacuum system as used in physical techniques, low cost, simple operations, high flexibility, and easy availability of equipment. This method widely used in many industrial applications.¹²

1.3 Metal Oxides

Metal oxide semiconductors role in photocatalysis have been studied extensively over the last few decades and they have proven to be good materials for environmental applications such as air and water purification, degradation of volatile organic compounds (VOCs) and disinfection. There are many metal oxides which have been used such as oxides of Ni, Co, Fe, Zr, Sn, Mg, Ti, Zn, etc. Due to its high electronegativity, oxygen forms stable chemical bonds with almost all elements to give the corresponding oxides. These can adopt a vast number of structural geometries with an electronic structure that can exhibit metallic, semiconductor or insulator characters. TiO_2 is well known as a cheap, nontoxic and efficient photocatalyst for the detoxication of air and water pollutants.¹⁰ TiO_2 occurs in three crystalline phases of anatase, rutile and brookite. The rutile phase of TiO_2 has a direct band gap value of 3.06 eV and an indirect band gap value of 3.10 eV while the band gap of anatase TiO_2 is 3.23 eV.¹³ In recent years literatures shows the photocatalytic activity of TiO_2 in degradation of various organic dyes such as Rhodamine B, Congo red and phenols.¹⁴

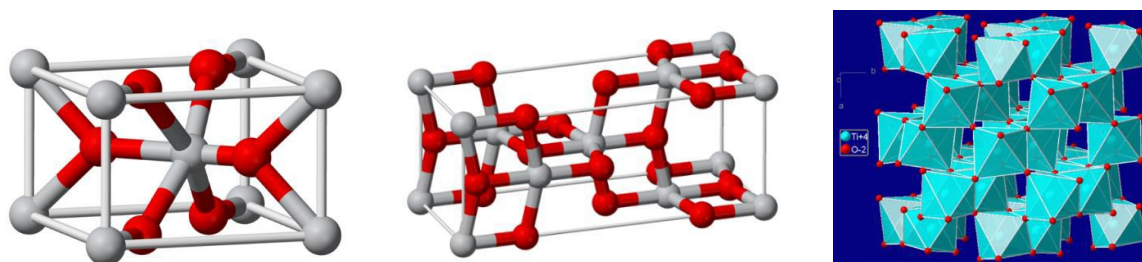


Fig. 2. Ball and stick model of crystal structures of i) Rutile, ii) Anatase and iii) Brookite TiO_2 .

1.3.1 Doping of Metal Oxides

The properties of these metal oxides in photocatalysis can be further exploited by suitable doping with metals and/non-metals to tune the band gap of the material to a specific range of frequencies of light. Recently, several attempts have been made by various groups to synthesize doped metal oxide structures to tune the band gap of the material to increase its activity in the visible region of light, such as the doping of carbon in TiO_2 ,¹⁵ nitrogen doped TiO_2 ,¹⁶ Pd doped TiO_2 .¹⁷ The doping of metals in these metal oxides are pre-dominantly monometallic nanoparticles.

1.4 Ionic Liquids

Ionic liquid can be defined as the family of the molten salts having melting point below 100 °C. They can be typically organic salts or eutectic mixtures of an organic salt and an

inorganic salt.¹⁸ Ionic liquid consists of exclusively or almost exclusively of ions. Water as a solvent has many drawbacks such as narrow liquid range of water (0-100 °C). Many organic solvents have low solubility in water. So water can't be used as a solvent for low and high temperature organic reactions. Organic solvents have low boiling points and high vapour pressure, the solubility of inorganic reactants in these solvents is low. Also, organic solvents are highly toxic, flammable and even explosive.¹⁸

The general properties of ionic liquid that make them suitable to chemical synthesis and catalysis include:¹⁸

- They have no (or negligible) vapour pressure and therefore do not evaporate.
- They have favourable thermal properties.
- They dissolve many metal complex, catalysts, organic compounds and gases.
- They are immiscible with many organic solvent and water.¹⁹

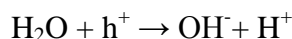
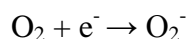
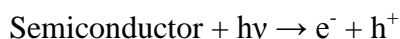
The different types of ionic liquids are

- Aprotic & protic (e.g. Ethylammonium nitrate ($[\text{C}_2\text{H}_5\text{NH}_3][\text{NO}_3]$) & 1-methylimidazolium tetrafluoroborate ($[\text{Hmim}][\text{BF}_4]$).
- Organic or Inorganic (e.g. 1-butyl-3-methylimidazolium bis (trifluoromethylsulfonyl) imide $[\text{C}_4\text{mim}][\text{NTf}_2]$ & Hydrazinium nitrate $[\text{N}_2\text{H}_5][\text{NO}_3]$).
- Task Specific (e.g. 1-Butyl-3-imidazolium cobalt tetra carbonyl $[\text{C}_4\text{mim}][\text{Co}(\text{CO})_4]$).
- Chiral (e.g. di(1-phenylethyl)imidazolium nitrate $[\text{dpeim}][\text{NO}_3]$)

1.5 Photocatalysis

Photocatalysis is the process by which, the rate of a reaction which occurs in the presence of light (photoreaction) is increased in the presence of a catalyst. A photocatalytic reaction can either be a homogenous or a heterogeneous reaction. The basic mechanism of a photocatalytic reaction involves the formation of electron-hole pairs, which is made possible by irradiating a semiconductor material with light which possesses an energy that is greater than the band gap of the material. The energy supplied is utilized by the electron to make a transition to the conduction band, which, in turn leaves a hole in the valence band. The efficiency with which a material can show photocatalytic activity depends on its ability to maintain charge separation of the generated electron-hole (e^-h^+) pairs by avoiding its

recombination, which enables the electrons and holes to migrate to the surface of the catalyst and take part in the reaction with adsorbed species. The electrons produced react with the oxygen molecule to form a superoxide anion (O_2^-) and the holes react with the water molecules adsorbed on the surface to produce the hydroxyl radical (OH^\cdot). The mechanism of a photocatalytic reaction can be summarized by the following equations:



Photocatalysis is one of the many available methods which can be used to degrade harmful organic compounds present in air and water, thus providing a simple method to purify air and water to eliminate the hazardous effects of pollution. The doping of some foreign cations may increase the activity of the photocatalyst and also modifies the microstructural property of the

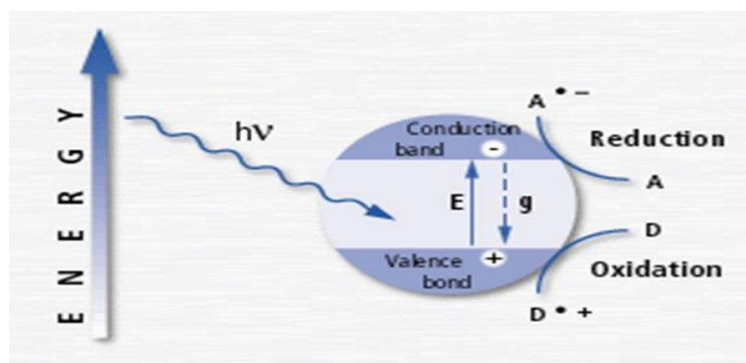


Fig. 3. Schematic diagram of a photocatalytic reaction.

catalyst. Many catalysts, besides the TiO_2 , like ZnO , ZrO_2 , WO_3 , SrO_2 , Fe_2O_3 , Nb_2O_5 , CeO_2 , CdS and ZnS have been attempted for the photocatalytic degradation of a wide variety of environmental contaminants.²⁰

1.6 Ionic Liquid for Metal Oxide Synthesis

The use of ionic liquids as media for the syntheses of various metallic nanoparticles has been reported in recent years.²¹ In addition to that ionic liquids have attracted a lot of interest as templates for the fabrication of nanostructured inorganic materials. Many porous inorganic oxide materials including zeolite materials, mesoporous silica with wormlike porous and highly ordered lamellar structures, mesoporous titania, and titania nanoparticles have been synthesized in ionic liquids.²² In all these cases, ionic liquid acts both as the solvent and the template. Recently use of ionic liquid for metal oxide synthesis has received more attention. Role of ionic liquid provide the convenient handling of larger spheres with a considerable

high surface area and narrow pore size distribution and are expected to have potential in solar energy conversion, catalysis, and optoelectronic devices.²³

1.7 Objectives of the Present Study

Photocatalytic activity of monometallic nanoparticles supported in metal oxides has been studied extensively and several research groups have reported an increase in the catalytic activity.²⁴ As ionic liquids can be used as novel media for the synthesis of both stable transition metal nanoparticles and porous inorganic materials, we were intrigued at the possibility of using ionic liquids for the incorporation of nanoparticles into porous oxide materials. The photocatalytic activity of nanoparticles supported in metal oxide such as TiO₂ in ionic liquid medium is relatively an unexplored field and to the best of our knowledge, not much work has been carried out to study photocatalysis using these supported materials. In this study, a novel supported nanoparticles system was synthesized in ionic liquid medium and the photocatalytic activities of these systems were studied. The main research objectives of the present study are:

- To synthesize, purify and characterize [BMIM]PF₆ ionic liquid.
- Incorporation of Ag nanoparticle in titania framework using ionic liquid via nanoparticle encapsulation process.
- To characterize supported metal oxide using UV-Vis, FTIR, SEM/EDX, and XRD.
- The photocatalytic activity measurement of the catalysts for the degradation of methylene blue under visible light.

Chapter-2

MATERIALS AND METHODS

2.1 Materials

1-methylimidazole (99%) and 1-chlorobutane (99.5%) was purchased from Sigma-Aldrich and was distilled over KOH and P₂O₅, respectively. Hexafluorophosphoric acid (ca. 65% solution in water), Silver nitrate (A.R.grade, 99% pure) (M.W.169.87 gmol⁻¹), sodium borohydride (M.W-37.83 g/mol), polyvinylpyrrolidone (PVP) (M.W-40,000), and Titanium isopropoxide were purchased from Sigma-Aldrich and were used without any further purification. The DI water used was Millipore water (18mΩ).

2.2 Synthesis

2.2.1 Synthesis of 1-butyl-3-methylimidazolium hexafluorophosphate [BMIM]PF₆ Ionic Liquid.

Before the synthesis of [BMIM]PF₆ ionic liquid, 1-butyl-3-methylimidazolium chloride (BMIMCl) ionic liquid was initially synthesized. The synthesis of BMIMCl was carried out according to the following procedure: To a 100 ml round bottom flask 1-methylimidazole (1.0 mol) was added in toluene (100 cm³) at 0 °C in vigorously stirred condition. After 5 min stirring, 1-chlorobutane (1.1 mol) was added and the solution was heated to reflux at 80 °C for 72 h under nitrogen atmosphere. The solution mixture was two phase layer one is the layer of BMIMCl and the other layer is toluene. Toluene was decanted. After toluene separation a crystalline solid of BMIMCl was obtained. Then the resulting product was recrystallized with acetone several times. Finally the resulting product was obtained. NMR was taken to check its purity and is shown in Fig (4). ¹H-NMR(CDCl₃, 400MHz): δ(ppm) = 10.52 (s, 1H, NCHN), 7.58 (m, 1H, CH₃NCHCHN), 7.43 (m, 1H, CH₃NCHCHN), 4.32 (t, 2H, NCH₃(CH₂)₂CH₃), 4.09 (s, 3H, NCH₃), 1.82 (m, 2H, NCH₂CH₂CH₂CH₃), 1.35 (m, 2H, N(CH₂)₂CH₂CH₃), 0.94 (t, 3H, N(CH₂)₃CH₃).

In a typical synthesis of 1-butyl-3-methylimidazolium hexafluorophosphate, BMIMCl (0.17 mol) was transferred to round bottom flask followed by the addition of 40 ml of deionized water. An aqueous solution of 65% HPF₆ in a 1.1:1 molar ratio was added slowly to minimize the amount of heat generated As HPF₆ was added two phases formed, where [BMIM]PF₆ was the bottom phase and the HCl was the upper phase. The upper phase was decanted and the remaining product was washed with water several times. Then the resulting product was dried

at 70 °C in vacuum line for 4 h to get the desired product. NMR spectra were shown in Fig (5). $^1\text{H-NMR}(\text{CDCl}_3, 400\text{MHz})$: $\delta(\text{ppm}) = 8.29$ (s, 1H, NCHN), 7.258 (d, 1H, CH_3NCHCHN), 7.22 (d, 1H, CH_3NCHCHN), 4.05 (m, 2H, $\text{NCH}_2(\text{CH}_2)_2\text{CH}_3$), 3.78 (s, 3H, NCH_3), 1.71 (m, 2H, $\text{NCH}_2\text{CH}_2\text{CH}_2\text{CH}_3$), 1.25 (m, 2H, $\text{N}(\text{CH}_2)_2\text{CH}_2\text{CH}_3$), 0.816 (t, 3H, $\text{N}(\text{CH}_2)_3\text{CH}_3$).

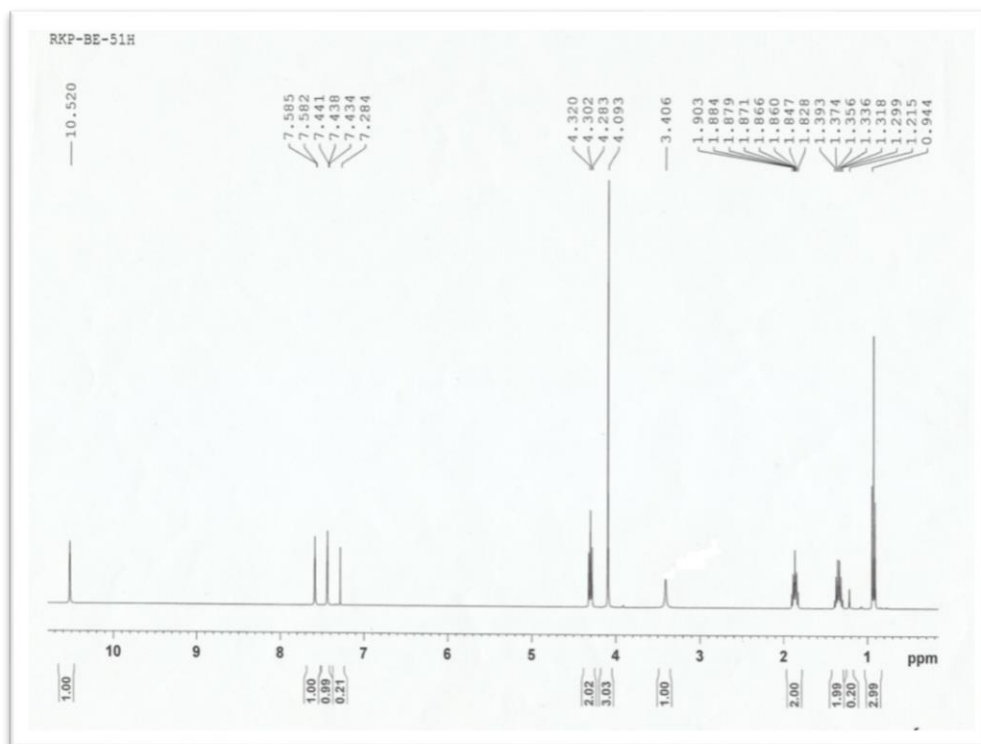


Fig. 4. NMR spectra of 1-butyl-3-methylimidazolium chloride.

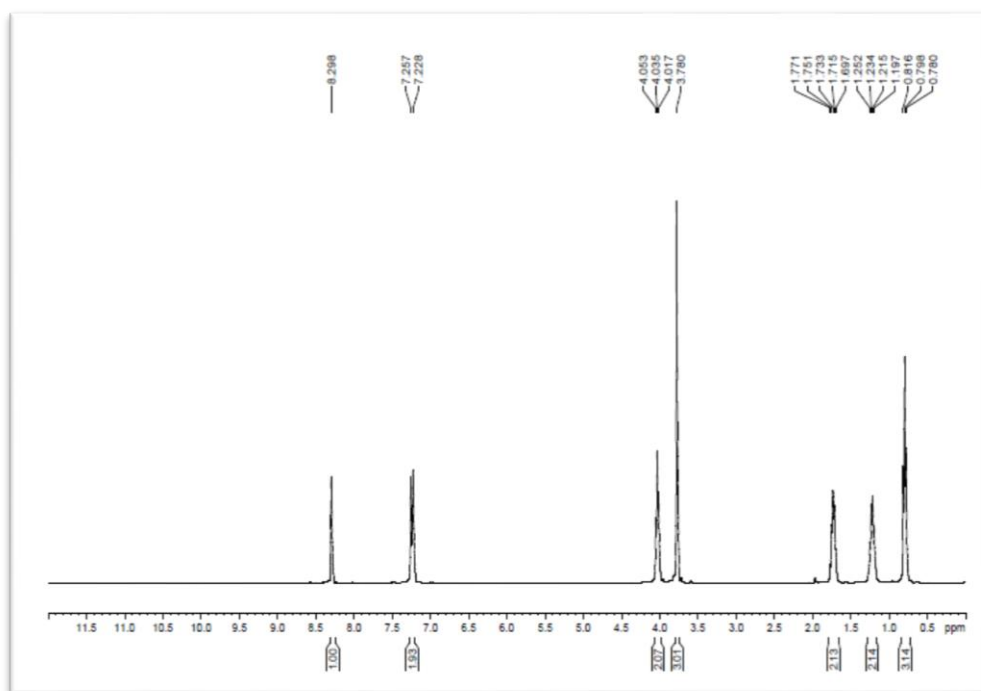


Fig. 5. NMR spectra of 1-butyl-3-methylimidazolium hexafluorophosphate.

2.2.2 Synthesis of Pure TiO₂ in [BMIM]PF₆ Ionic Liquid

5 mL of methanol was taken in a beaker and 0.25 mL (5 vol. %) of water was added to it and stirred. After that 2.02 mL of Ti(OⁱPr)₄ was added to 5 ml of hot methanol dried using molecular sieves. Solution of titanium precursor was added to a beaker followed by addition of 3 ml of ionic liquid within 5-10 sec a gel was formed. Then it was left to age overnight and followed by drying at a temperature of 150-200 °C for 1-2 h. The dried gel was then powdered using a mortar and pestle and calcined in air at a temperature of 450 °C for 3 h. Titania thus obtained was characterized using various characterization technique and its properties of photocatalysis was studied.

2.2.3 Synthesis of Ag-Doped TiO₂ in [BMIM]PF₆ Ionic Liquid

Silver nanoparticle was synthesized in methanol by taking 0.011 mmol of AgNO₃ as the precursor salt. This was added to 5 mL of methanol and stirred continuously with 0.0056 mmol of PVP as the stabilizing agent. After a few minutes, 0.11 mmol of NaBH₄ were added to reduce the metal ions and a yellow solution was obtained indicating the formation of Ag nanoparticles.

Later on these silver nanoparticles are incorporated into titania by using nanoparticle encapsulation method. The prepared monometallic nanoparticle solutions of Ag was taken in a beaker and 0.25 mL (5 vol. %) of water was added to it and stirred. 2.02 mL of Ti(OⁱPr)₄ taken as the titanium precursor was added to 5 mL of hot methanol dried using molecular sieves. Addition of titanium precursor was followed by addition of 3 mL of [BMIM]PF₆ ionic liquid. A gel was formed in 5-10 seconds. This was then left to age overnight and followed by drying at a temperature of 150-200 °C for 1-2 h. The dried gel was then powdered using a mortar and pestle and calcined in air at a temperature of 450 °C for 3 h. The monometallic nanoparticles doped in titania thus obtained, were characterized and its properties of photocatalysis were studied.

2.2 Photocatalytic studies

2.2.1 Instrumentation

Photocatalytic studies were conducted in a dark reaction chamber (50 cm x 50 cm x 50 cm) and an artificial sunlight setup was used. The source of light used for visible radiation was a Bajaj, high pressure mercury vapour (HPMV) lamp, 125 W, 220-250 V with peak emission at a wavelength of about 450 nm. The distance between the lamp and the surface of the solution was about 15 cm.

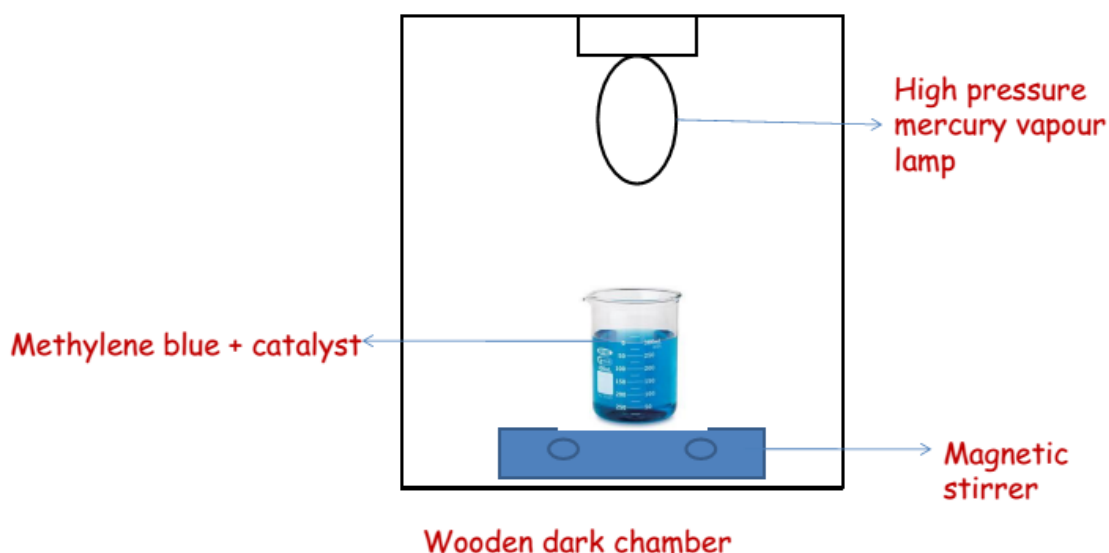


Fig. 6. Photocatalysis set-up

2.2.2 Photocatalysis Measurements

The photocatalytic measurements were carried out by the degradation rate of Methylene Blue (MB) dye. A known concentration of the dye was prepared (20 ppm) and its spectra were obtained before the addition of catalyst. The spectra indicated the MB absorption before the catalyst addition. Then 100 mg of catalyst was to the MB solution and it was stirred in the dark for 30 min to obtain photocatalyst-dye equilibrium. A small quantity was then taken out with a syringe and was centrifuged at 8,000 rpm for 10 min to remove the catalyst. The supernatant was taken and filled in a quartz cuvette without dilution and was studied using UV-Vis spectroscopy to calculate the concentration of MB dye. This was performed in order to determine the effect of MB adsorption on the photocatalyst material. The concentration measured was taken as MB concentration at 0 min at which photocatalysis occurs. The solution was stirred using a magnetic stirrer for 30 min and a sample was withdrawn and the UV-Vis spectra was obtained. The similar process was carried out and the sample was collected at an interval of 30 min for two hours. The concentration of MB was determined and the rate of degradation was calculated.

2.4 Characterization of Catalysts

The materials synthesized in the above sections were characterized by UV-Visible spectroscopy (UV-Vis), Infra-Red Spectroscopy (IR), X-Ray diffraction (XRD), Scanning Electron Microscopy (SEM), to check purity of ionic liquid; Nuclear Magnetic Resonance (NMR) was taken.

UV-Vis Spectroscopy

UV-Vis Spectra of pure ionic liquid [BMIM]PF₆ were recorded by Shimadzu spectrophotometer (UV-2450) in the range of 200-900 nm. Photocatalytic activity of the prepared catalysts was also measured using UV-Vis spectroscopy.

Infrared Spectroscopy (IR)

The IR spectra of pure TiO₂ and Ag-doped TiO₂ in ionic liquid after calcination were recorded using Perkin-Elmer infrared spectrometer with a resolution of 4 cm⁻¹, in the range of 400 cm⁻¹ to 4000 cm⁻¹. Nearly 3-4 mg of the sample was mixed thoroughly with 30 mg of oven dried KBr and made into pellets.

X-ray diffraction (XRD)

The X-ray diffraction patterns of the pure TiO₂ and Ag-doped TiO₂ were recorded on a Phillips PAN analytical diffractometer using Ni-filtered CuK_{α1} radiation. The XRD measurements were carried out 20-80 degree for both the samples, respectively with a scan speed of 5 degrees per minute.

Scanning Electron Microscopy (SEM)/ Energy dispersive X-ray spectroscopy (EDX)

Scanning electron microscopy was taken using JEOL JSM-6480 LV microscope (acceleration voltage 15 kV). The sample powders were deposited on a carbon tape before mounting on a sample holder for SEM analysis. EDX analysis shows the presence of Ag nanoparticles on titania framework.

Chapter-3

RESULTS AND DISCUSSION

3.1 UV-Visible study

The UV-Vis spectra of the pure ionic liquid (1-butyl-3-methylimidazolium hexafluorophosphate) in the scanning range 200-800 nm is shown in Fig 7. To minimise the effect of impurities on ionic liquid, it was recrystallized in acetone three times and were washed with water. In order to see whether colored impurities were still present or not, UV-Vis spectra were taken. No absorption peak was observed which confirmed the formation of impurity free ionic liquid.

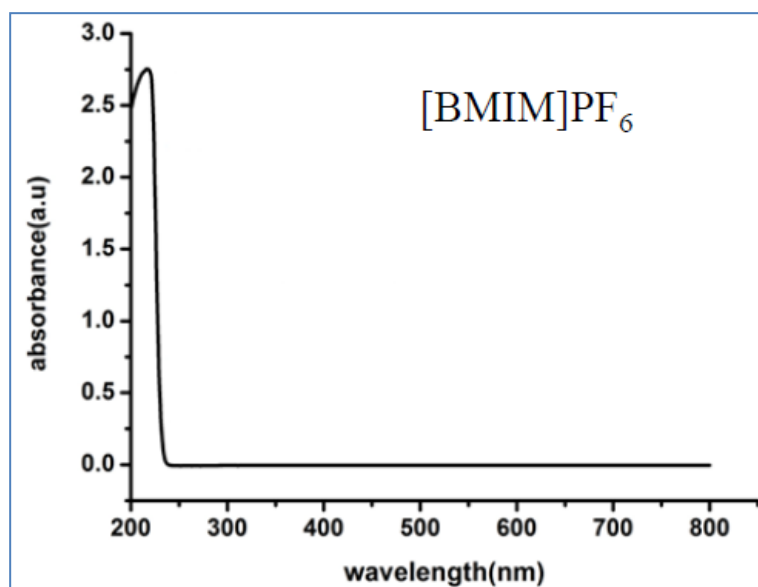


Fig. 7. UV-Vis spectra of 1-butyl-3-methylimidazolium hexafluorophosphate ionic liquid.

3.2 FTIR Study

The Fourier Transform Infrared (FTIR) spectra of the samples are shown in Fig 8. The peak centered at around 3400 cm^{-1} indicates the presence of water molecules and the OH stretching mode which occurs in the range of $3400 - 3000\text{ cm}^{-1}$. The peak around 1200 cm^{-1} indicates the C-O bond, usually observed in the range of $1260 - 1000\text{ cm}^{-1}$, is formed due to metal-carbonyl linkages possibly caused by adsorption of CO from atmosphere.^{24d} The range of wavenumber from $1000 - 400\text{ cm}^{-1}$ is called the fingerprint region and in the above graph, the broad peak in the range of $1000 - 400\text{ cm}^{-1}$ is caused by overlapping of peaks of

the Ti-O and Ti-O-Ti stretching mode obtained at various values of wavenumbers at around 400 cm^{-1} , 460 cm^{-1} , 700 cm^{-1} and 750 cm^{-1} .

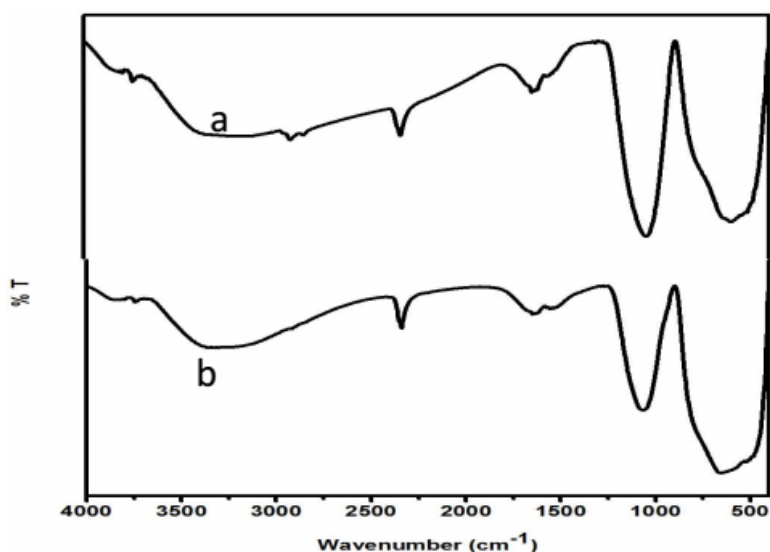


Fig. 8. FTIR of (a) Ag-doped TiO_2 , and (b) Pure TiO_2 in $[\text{BMIM}]\text{PF}_6$ ionic liquid

This broad peak indicates the metal-oxygen bonds, i.e. the Ti-O-Ti or Ti-O vibration mode.²⁵

3.3 SEM/EDX study

The SEM analysis was carried out to study the compositional analysis of the supported oxides and the elemental analysis was carried out with EDX. Fig 9 shows the SEM and EDX spectra of pure TiO_2 which was synthesized in ionic liquid medium, the morphology of TiO_2 particles seems to be spherical in shape and are uniformly distributed. The EDX was recorded in the binding energy region of 20 keV. The chemical composition analysis shows the presence of Ti (highly intense) and O. Presence of Au is due to coating which was done to make a sample conducting.

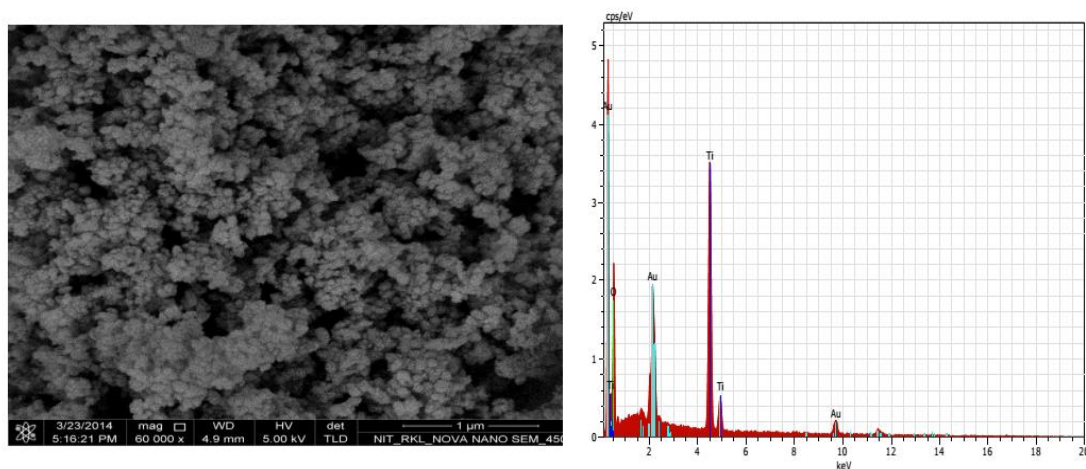


Fig. 9. SEM/EDX spectra of Pure TiO_2 in $[\text{BMIM}]\text{PF}_6$ ionic liquid.

Fig 10 shows the SEM and EDX image of Ag-doped titania in ionic liquid medium. As compared to the SEM image of pure titania in ionic liquid Ag-doped titania exhibited much

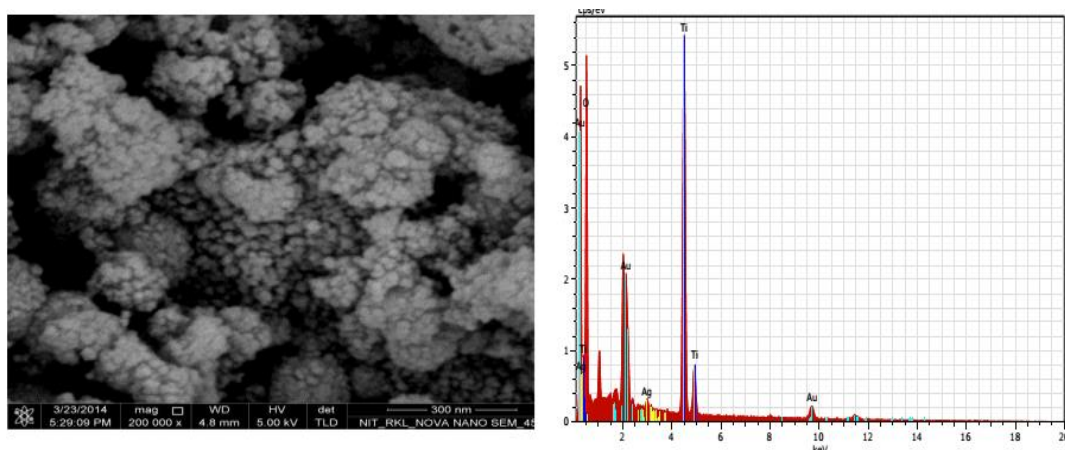


Fig. 10. SEM/EDX spectra of Ag-doped TiO₂ in [BMIM]PF₆ ionic liquid.

rough surface which is due to phase separation of silver species.²⁶ The peak from the EDX spectrum reveals the presence of three peaks at around 0.5 keV, 4.5 keV and 5 keV, respectively. The intense peak is assigned to the bulk Ti and O. The peaks of Ag are at 0.2 keV and 3 keV. This result confirms the existence of Ag nanoparticles in TiO₂ matrix.

3.4 XRD study

The XRD pattern of pure titania and Ag-doped titania synthesized in ionic liquid medium was shown in Fig 11(a and b). The X-ray diffraction pattern shows the peak at 2 θ values of 25.2° corresponds to [101] crystal planes of anatase TiO₂ which matches well to the reported JCPDS data (Card No. 71-1166).

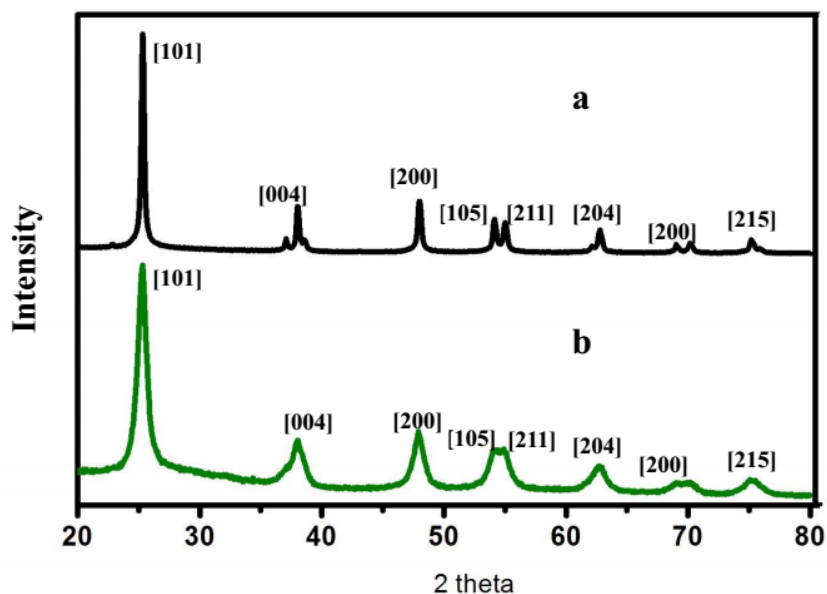


Fig. 11. XRD plot of (a) Pure TiO₂, and (b) Ag-doped TiO₂ in [BMIM]PF₆ ionic liquid.

The XRD of silver doped titania samples coincides with that of pure titania and show no diffraction peaks due to the presence of silver species, which suggest that the Ag nanoparticles are well dispersed in TiO₂ surface. Also, absence of XRD peaks due to the polycrystalline silver can be attributed to the low Ag loading (~ 1 wt. %) and the presence of very small silver nanoparticles dispersed on the titania matrix. As from XRD pattern it shows that doping with Ag on titania does not disturb the crystal structure of anatase titania indicating that the metal dopant are merely placed on the surface of the crystal without being covalently anchored into the crystal lattice.²⁷ The commercial phase of titania is anatase phase which preferably shows higher photocatalytic activity in comparison to rutile and brookite phase.

3.5 Photocatalysis

Fig 12 (a) depicts the absorption spectra of Ag-doped TiO₂ synthesized using ionic liquid medium via nanoparticle encapsulation method. The spectra show the photocatalytic degradation of 20 mg/L methylene blue dye in 100 mg of photocatalyst in aqueous solution under the irradiation of visible light. Fig 12 (a) displays the absorption band of MB at around 652 nm and the peak intensity rapidly decreased in 210 min under visible light. To compare the activity of our Ag-doped TiO₂ catalysts synthesized in ionic liquid, the photocatalytic activity of our catalyst was compared with Ag-doped titania synthesized using common organic solvent such as in methanol. Fig 12 (b) shows the absorption peak of degradation of methylene blue over supported titania in methanol solvent.

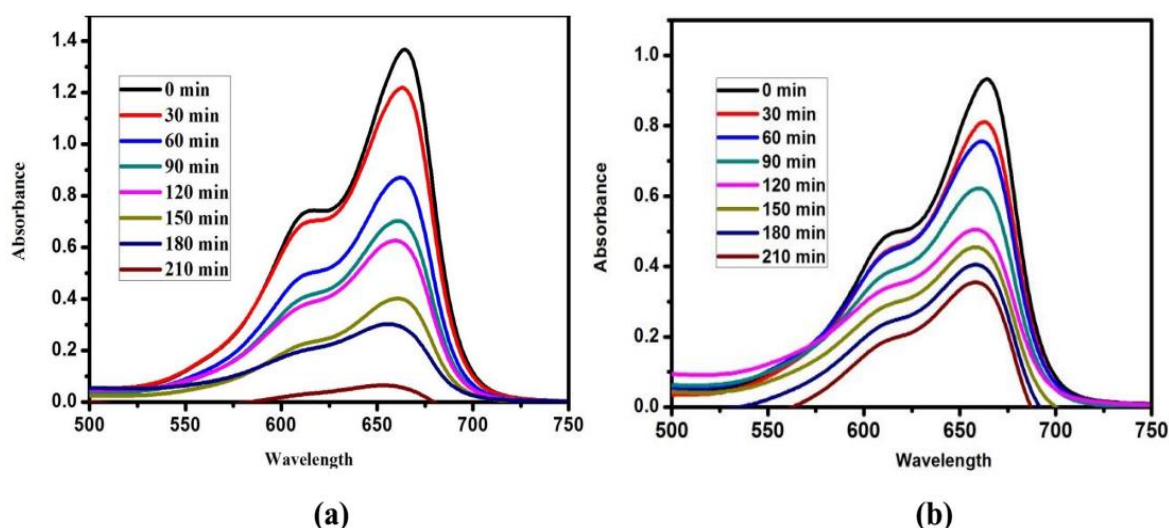


Fig. 12. Photocatalytic degradation of methylene blue over (a) Ag-doped TiO₂ in [BMIM]PF₆ ionic liquid, and (b) Ag-doped TiO₂ in methanol medium.

It was observed that Ag-doped TiO₂ in ionic liquid shows much faster degradation rate compare to Ag-doped TiO₂ in methanol and also pure titania in ionic liquid. After 210 min it was observed that Ag-doped TiO₂ in ionic liquid shows around 96 % of degradation compare to which Ag-doped TiO₂ in methanol shows 65 % of degradation. The higher activity can be attributed to the formation of highly porous titania using ionic liquid as a novel medium. Scott and co-workers have demonstrated the formation of highly porous materials in ionic liquid compared that in methanol solvent.²⁸ Highly mesoporous titania (BET surface area of 200 m²/g, pore size of 3-5 nm, and pore volume of 0.69 cm³/g) with anatase crystalline phase was obtained by calcination at 350 °C using [BMIM]PF₆ ionic liquid. They postulated that the PVP template plays a dual role as a template for both nanoparticle formation and as a porogen for the final titania sol-gel materials. Thus, presence of ionic liquid and PVP play a very important role in the final structure of titania.

Fig 13 shows the colour change of 20 mg/L methylene blue dye in presence of 100 mg of Ag-doped TiO₂ photocatalyst after regular interval of time under visible light irradiation. Complete decolourisation of MB in presence of Ag-doped TiO₂ was achieved with 210 min.

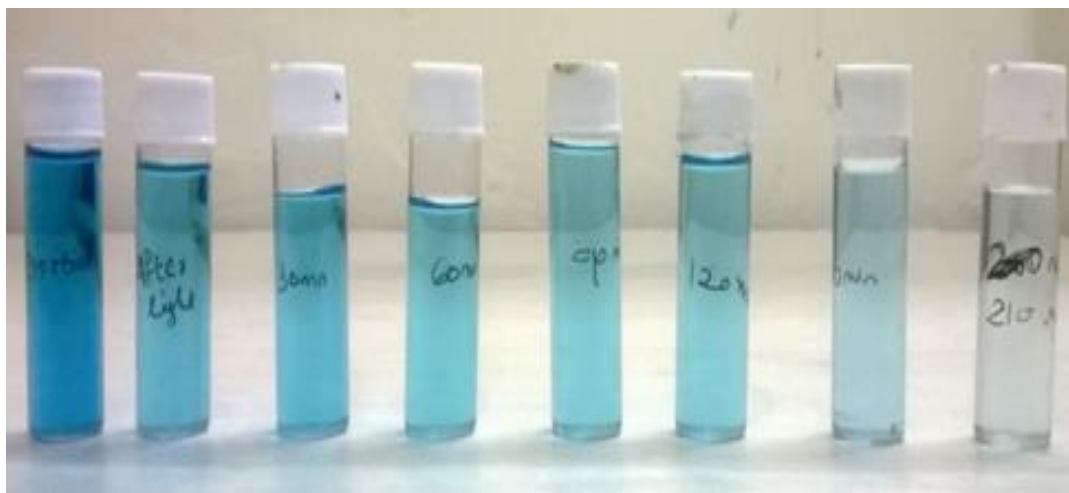


Fig. 13. Change in colour of methylene blue after degradation under visible light using Ag-dopedTiO₂ catalyst.

The result indicates that Ag-doped titania in ionic liquid serves as a good photocatalyst for degradation of methylene blue.

Chapter-4

CONCLUSIONS AND FUTURE WORK

Ag-doped in TiO₂ was successfully synthesized by the nanoparticle encapsulation method using ionic liquid medium. The FTIR studies confirmed the presence of Ti and O bonds in the samples. The XRD studies revealed that the TiO₂ synthesized had an anatase crystal structure. The nanoparticles were found to be of spherical shape. EDX spectra showed the presence of Ag nanoparticle on TiO₂ framework. The PVP template during the synthesis plays a dual role as a template for both nanoparticle formation and as a porogen for the final titania sol-gel materials. The Ag-doped in TiO₂ was found to be an effective photocatalyst with a photocatalytic efficiency of almost 96 % in visible light for the degradation of methylene blue compared to the Ag-doped in TiO₂ synthesized in methanol solvent where 65 % degradation was achieved in the specified time.

As Ag-doped titania has been synthesized successfully using ionic liquid, further studies will investigate the synthesis of supported bimetallic nanoparticles. One possible direction of the research would be the synthesis of bimetallic nanoparticle doped titania in ionic liquid and their application in degradation of organic dyes and phenols.

Chapter 5

REFERENCES

1. Anthony, J. L.; Maginn, E. J.; Brennecke, J. F., *Journal of Physical Chemistry:B* **2002**, *106*, 7315-20.
2. Antonietti, M.; Kuang, D. B.; Smarsly, B.; Yong, Z., *Angewandte Chemie, International Edition* **2004**, *43*, 4988–4992.
3. Tian, N.; Zhou, Z. Y.; Sun, S. G., *Journal of Physical Chemistry: C* **2008**, *112*, 19801-17.
4. Park, Y. J.; Lee, H. I., *Journal of Nanomaterials* **2014**, *2014*, 1-6.
5. Choi, H.; Kim, Y. J.; Varma, R. S.; Dionysiou, D. D., *Chemistry of Materials* **2006**, *18*, 5377-5384.
6. Ahmed, M. A.; Katori, E. E. E.; Gharni, H. Z., *Journal of Alloys and Compounds* **2013**, *553*, 19-29.
7. Didier, A.; Feng, L.; Jaime, R. A., *Angewandte Chemie, International Edition* **2005**, *44*, 7852-7872.
8. Naoki, T.; Tetsu, Y., *New Journal of Chemistry* **1998**, *22*, 1179-1201.
9. Faraday, M. P., *Transaction of Royal Society* **1857**, *147*, 145-181.
10. Qamar, M.; Muneer, M., *Desalination* **2009**, *249*, 535-540.
11. Samuel, R. A.; Yijun, G. T.; Purnima, A.; Andreja, B.; Javier, V., *Journal of Physical Chemistry: C* **2012**, *116*, 10382-10389.
12. Raja, M.; Subha, J.; Binti, F.; Ryu, S., *Materials and Manufacturing Process* **2008**, *23*, 782-785.
13. (a) Hoffmann, M. R.; Martin, S. T.; Choi, W. Y.; Bahnemann, D. W., *Chemical Reviews* **1995**, *95*, 69-96; (b) Yu, J. G.; Su, Y. R.; Cheng, B., *Advanced Functional Materials* **2007**, *17*, 1984-1990; (c) Yu, H. G.; Yu, J. G.; Liu, S. W.; Mann, S., *Chemistry of Materials* **2007**, *19*, 4327-4334; (d) Jing, L.; Wang, D.; Wang, B.; Li, S.; Xin, B.; Fu, H.; Sun, J., *Journal of Molecular Catalysis: A* **2006**, *244*, 193-200; (e) Stroyuk, A. L.; Shvalagin, V. V.; Kuchmii, S. Y., *Journal of Photochemistry and Photobiology: A* **2005**, *173*, 185-194; (f) Yu, J. G.; Zhang, L. J.; Cheng, B.; Su, Y. R., *Journal of Physical Chemistry: C* **2007**, *111*, 10582-10589; (g) Yu, J. G.; Liu, S. W.; Yu, H. G., *Journal of Catalysis* **2007**, *249*, 59-66.
14. Sclafani, A.; Palmisano, L.; Schiavello, M., *Journal of Physical Chemistry* **1990**, *94*, 829-832.

15. Song, K.; Zhou, J.; Bao, J.; Feng, Y., *Journal of American Ceramic Society* **2008**, *91*, 1369-1371.
16. Wu, Y.; Liu, H.; Zhang, J.; Chen, F., *Journal of Physical Chemistry: C* **2009**, *113*, 14689-14695.
17. EI-Rady, A. A. A.; EI-Sadek, A. S. M.; EI-Sayed Breky, M. M.; Assaf, H. F., *Advances in Nanomaterials* **2013**, *2*, 372-377.
18. Zhen, M.; Jihong, Y.; Sheng, D., *Advanced Materials* **2010**, *22*, 261-285.
19. Paul, J. D., *Organometallic Chemistry* **2002**, *16*, 495-500.
20. Gopal, V. K.; Kamat, P. V., *Environmental Science and Technology* **1995**, *29*, 841-845.
21. Migowski, P.; Dupont, J., *Chemistry - A European Journal* **2007**, *13*, 32-39.
22. Ma, Z.; Yu, J. H.; Dai, S., *Advanced Materials* **2010**, *22*, 261-285.
23. Zhou, Y.; Antonietti, M., *Journal of American Chemical Society* **2003**, *125*, 14960-14961.
24. (a) Wawrzyniak, B.; Morawski, A. W., *Applied Catalysis B: Environmental* **2006**, *62*, 150-158; (b) Iliev, V.; Tomova, D.; Bilyarska, L.; Petrov, L., *Catalysis Communications* **2004**, *5*, 759-772; (c) Nakajima, A.; Obata, H.; Kameshima, Y.; Okada, K., *Catalysis Communications* **2005**, *6*, 716-720; (d) Mei, L.; Liang, K.; Wang, H., *Catalysis Communications* **2007**, *8*, 1187-1199; (e) Morawski, A. W.; Janus, M., *Polish Journal of Chemical Technology* **2005**, *7*, 81-86.
25. Castellano, F. N.; Stipkala, J. M.; Friedman, L. A.; Meyer, G. L., *Chemistry of Materials* **1994**, *6*, 2123-2129.
26. Liu, H.; Dong, X.; Liu, T.; Duan, C.; Zhu, Z., *Materials Letters* **2013**, *110*, 111-113.
27. Nainani, R.; Thakur, P.; Chaskar, M., *Journal of Materials Science and Engineering :B* **2012**, *2*, 52-58.
28. Dash, P.; Scott, J. W. R., *Materials Letters* **2011**, *65*, 7-9.